Staphylococcus pseudintermedius Surface Protein L (SpsL) Is Required for Abscess Formation in a Murine Cutaneous Infection Model

Staphylococcus pseudintermedius Surface Protein L (SpsL) Is Required for Abscess Formation in a Murine Cutaneous Infection Model

Amy C. Richards, Marie O'Shea, Philippa M. Beard*, Mariya I. Goncheva*, Stephen W. Tuffs*, J. Ross Fitzgerald#, Andreas Lengeling*#

The Roslin Institute, Royal (Dick) School of Veterinary Sciences, University of Edinburgh, UK

Running Title: SpsL is required for Abscess Formation

Keywords: *Staphylococcus pseudintermedius*, abscess, cellulitis, skin infection

#Address correspondence to J. Ross Fitzgerald, ross.fitzgerald@roslin.ed.ac.uk, and Andreas Lengeling, andreas.lengeling@gv.mpg.de

*Present address: Philippa M. Beard, The Pirbright Institue, Surrey, UK
Mariya I. Goncheva, Department of Microbiology and Immunology, Schulich School of Medicine and Dentistry, Western University, London, Ontario, Canada
Stephen W. Tuffs, Department of Microbiology and Immunology, Schulich School of Medicine and Dentistry, Western University, London, Ontario, Canada
Andreas Lengeling, Max-Planck-Society – Administrative Headquarters, Munich, Germany

Abstract

Staphylococcus pseudintermedius is the leading cause of pyoderma in dogs and is often associated with recurrent skin infections that require prolonged antibiotic therapy. High levels of antibiotic use have led to multidrug resistance including the emergence of epidemic methicillin-resistant clones. Our understanding of the pathogenesis of *S. pseudintermedius* skin infection is very limited and the identification of the key host-pathogen interactions underpinning infection could lead to the design of novel therapeutic or vaccine-based approaches for controlling disease. Here, we employ a novel murine cutaneous infection model of *S. pseudintermedius* and investigate the role of the two cell wall-associated proteins (SpsD and SpsL) in skin disease pathogenesis. Experimental infection with wildtype *S. pseudintermedius* strain ED99, or a gene-deletion derivative deficient in expression of SpsD, led to a focal accumulation of neutrophils and necrotic debris in the dermis and deeper tissues of the skin, characteristic of a classical cutaneous abscess. In contrast, mice infected with mutants deficient in SpsL or both SpsD and SpsL developed larger cutaneous lesions with distinct histopathological features of regionally extensive cellulitis rather than focal abscessation. Furthermore, comparison of the bacterial load in *S. pseudintermedius*-induced cutaneous lesions revealed a significantly increased burden of bacteria in the mice infected with SpsL-deficient mutants. These findings reveal a key role for SpsL in murine skin abscess formation and highlight a novel function for a bacterial surface protein in determining the clinical outcome and pathology of infection caused by a major canine pathogen.

Introduction

Staphylococcus pseudintermedius, a coagulase-positive species, is a natural commensal of the skin and mucosal membranes of dogs with healthy carriage rates reported to range from 46% - 92% (1). *S. pseudintermedius* is capable of causing a range of opportunistic infections including urinary tract, ear, wound, and surgery-related infections (1). The most clinically important consequence of *S. pseudintermedius* infection is canine pyoderma with approximately 10% of dogs affected worldwide (2). Canine pyoderma is an umbrella term used to describe a range of clinical manifestations, most commonly superficial bacterial folliculitis and atopic dermatitis, which are often treated with antibiotics alongside topical creams and shampoos containing antimicrobial agents such as chlorhexidine (3, 4). The repeated use of antibiotics in patients with recurrent pyoderma is linked to the development of antibiotic resistance and the rapid global spread of methicillin resistant *S. pseudintermedius* (MRSP), with some strains developing resistance to all commonly used antimicrobials in veterinary medicine (5-8). The high prevalence of multidrug resistant *S. pseudintermedius* is a major concern for the continued treatment of canine pyoderma.

Our understanding of the pathogenesis of *S. pseudintermedius* infection and the key bacterial factors involved is very limited. Exfoliative toxins ExpA and ExpB, cause intra-epidermal clefts in the skin by directly cleaving canine desmoglein 1 and both intradermal and subcutaneous injection of either exfoliative toxin, in dogs, leads to the development of clinical manifestations of pyoderma including crusting and erythema (9-11). Bacterial adhesins are also thought to be important as the *S. pseudintermedius* clinical isolate ED99 demonstrates increased adherence to pyoderma-associated canine corneocytes when compared with healthy corneocytes (12). Of the 18 cell wall-associated (CWA) proteins encoded in the genome sequence of *S. pseudintermedius* clinical isolate ED99, two have been demonstrated to mediate binding to host proteins (13). *S. pseudintermedius* surface proteins D and L (SpsD and SpsL), mediate binding to the host extracellular matrix proteins

fibrinogen, fibronectin, and the cytoskeletal protein cytokeratin-10 when expressed by the heterologous host *Lactococcus lactis* (13). Recombinant versions of the SpsD N-terminal A-domain interfere with fibrin clot formation and platelet aggregation *in vitro* and both SpsD and SpsL are sufficient for the invasion of *S. pseudintermedius* into canine progenitor epidermal keratinocytes in a fibronectin-dependent manner *in vitro* (14, 15). To date, the role of *S. pseudintermedius* putative virulence factors have not been examined during experimental infection.

Skin infection models have been employed previously to analyse the role of CWA proteins of *Staphylococcus aureus* by subcutaneous injection of wildtype and gene deletion strains (16-18). In these studies, mice develop focal skin abscesses and dermonecrosis within 24 h that subsequently resolve spontaneously after 14 d in the absence of a systemic response (16). These skin lesions can be evaluated using histopathology or homogenised to determine the number of viable bacteria present. Here we develop the first murine infection model of *S. pseudintermedius* and assess the role of SpsD and SpsL in this murine model using single and double deletion strains of *spsD* and *spsL* in the *S. pseudintermedius* clinical isolate ED99, originally isolated in the UK from a dog affected by canine pyoderma (12). We discovered that the wildtype and *spsD*-deficient-infected mice developed classical abscessation near the inoculation site. In contrast, mice inoculated with *spsL*-deficient or *spsLspsD*-deficient strains, developed an alternative clinical pathology described as cellulitis. These findings demonstrate that a bacterial CWA protein determines the clinical outcome of infection in a novel murine cutaneous model.

Results

SpsD and SpsL of *S. pseudintermedius* ED99 Adhere to Murine Fibronectin, Fibrinogen, and Cytokeratin-10. Previous work demonstrated that *S. pseudintermedius* SpsD and

SpsL can mediate binding to extracellular matrix proteins fibronectin and fibrinogen and the cytoskeletal protein cytokeratin-10, when expressed on the surface of a heterologous host *L. lactis* (2). To determine if murine skin was a suitable model for the analysis of SpsD and SpsL, we examined their capacity to mediate binding to the murine proteins fibronectin, fibrinogen, and cytokeratin-10. The expression of SpsD and SpsL on the surface of *L. lactis* mediated binding to murine fibronectin, fibrinogen, and cytokeratin-10, with SpsD demonstrating stronger binding to murine cytokeratin-10 and fibrinogen than SpsL (Fig. 1A and B). This suggests that the role of SpsD and SpsL in the pathogenesis of *S. pseudintermedius* canine pyoderma can be examined in a murine infection model.

In order to examine the importance of SpsD and SpsL in mediating binding of *S. pseudintermedius* ED99 to the same murine ligands, we performed solid phase bacterial adherence assays with wildtype, and single or double *spsL* and *spsD* deletion mutants (15). Expression analysis demonstrated that SpsD is expressed on the cell surface at early exponential phase (OD_{600} of 0.2) with SpsL expressed on the cell surface throughout the exponential phase (data not shown). Accordingly, the binding potential of CWA SpsD and SpsL were investigated by solid phase adherence assays at early exponential growth phase. As expected, *S. pseudintermedius* ED99 demonstrated adherence to murine fibronectin, murine fibrinogen, and murine cytokeratin-10 (Fig. 1C-1E). Equivalent murine fibronectin binding to the wildtype was observed for ED99Δ*spsD* demonstrating that SpsL is promoting binding to fibronectin (Fig. 1C). However, ED99Δ*spsL* retains a reduced adherence to fibronectin demonstrating that SpsD is sufficient for fibronectin-binding (Fig. 1C). Adherence to murine fibrinogen was reduced in comparison to the other ligands with both ED99Δ*spsD* and ED99Δ*spsL* exhibiting reduced binding suggesting that both SpsL and SpsD, respectively, are capable of mediating adherence to murine fibrinogen (Fig. 1D). Surprisingly, ED99Δ*spsL* exhibits poor binding to cytokeratin-10 suggesting that SpsL is the main mediator of cytokeratin-10 binding (Fig. 1E). Of note, ED99Δ*spsL*Δ*spsD* demonstrated complete

ablation of binding to all three ligands confirming that SpsD and SpsL are the only CWA proteins of *S. pseudintermedius* ED99 promoting adherence to murine fibronectin, fibrinogen, and cytokeratin-10 under these assay conditions (Fig. 1A-C).

Development of a Murine Cutaneous Infection Model of *S. pseudintermedius* ED99. Initially, pilot experiments were performed to develop the first murine skin infection model of *S. pseudintermedius*. Female BALB/c mice received an injection of either 100 µl volume PBS or $1x10^7$ CFU of *S. pseudintermedius* ED99 (in 100 µl PBS) as a bolus into the subcutaneous tissue of the dorsal midline, just caudal to the interscapular region. Mice were then monitored for 4 d post-infection (dpi) to determine the severity of the disease and follow the development of skin lesions. The wildtype-infected mice exhibited a trend towards greater weight loss than the control mice but this was not significant suggesting that a systemic infection did not occur (Fig. 2A), and there were no differences in the size of excised spleens (Fig. S1A). Cutaneous lesions in the wildtype-infected mice became visible on the back or flank of the mouse at 2 dpi and became more prominent by 4 dpi (Fig. 2B). The gross pathology was typified by a soft cutaneous lesion of varying shape up to 9 mm along the longest axis, unattached to the underlying tissue, and with a well-defined, reddened margin. On the cut surface there were one or 2 circumscribed, round, soft to liquid areas (pus) approximately 1-2 mm diameter within the dermis and subcutis underlying the lesion.

A subset of mice were euthanised at 1, 2, and 4 dpi and the dorsal cutaneous tissue excised, fixed in 10 % formal saline and processed using standard procedures to tissue sections which were then stained with haematoxylin and eosin and examined by a veterinary pathologist (P.M.B). No significant pathology was identified in the tissue from the control mice (Fig. 2C). Wildtype-infected mice developed classic skin abscesses characterised by a focal accumulation of neutrophils (some degenerate), cellular debris and bacteria (Fig. 2D), with no appreciable differences in size or disease severity over time (Fig. S1 B and C). This pilot study demonstrated that *S. pseudintermedius*-

157 infected mice develop classic cutaneous abscesses similar to those clinically described in dogs
158 affected by *S. pseudintermedius* pyoderma (3).

159 **Infection with *S. pseudintermedius* Lacking SpsD and SpsL Cell Wall-associated**
160 **Proteins Results in a Distinct Skin Infection Pathology.** The murine *S. pseudintermedius* skin
161 infection model was used to determine the role of bacterial CWA proteins in the pathogenesis of
162 cutaneous infection. Female BALB/c mice were injected subcutaneously as described previously
163 with either *S. pseudintermedius* wildtype or the derivative ED99Δ*spsL*Δ*spsD* deletion mutant and
164 monitored for 3 dpi. The mice infected with the ED99Δ*spsL*Δ*spsD* strain lost more body weight
165 than the mice infected with the wildtype strain at all three time points ($p \leq 0.05$ at 2 dpi) (Fig. 3A).
166 Gross examination of the site of inoculation revealed that the wildtype-infected mice developed
167 raised, soft cutaneous lesions with a reddened margin similar to those described in the pilot
168 experiments above. In comparison, ED99Δ*spsL*Δ*spsD*-infected mice developed flattened,
169 longitudinally extended cutaneous lesions that covered a larger area (Fig. S2). Measurement of the
170 cutaneous lesions along the longest axis confirmed that ED99Δ*spsL*ΔspsD-infected mice develop
171 significantly longer lesions than wildtype-infected mice at both 2 and 3 dpi ($p \leq 0.001$) (Fig. 3B).
172 Histopathological examination of the inoculated area in mice infected with the wildtype strain
173 revealed the presence of focal, well circumscribed abscesses consistent with that observed in the
174 pilot study (Fig. 3C). However, focal abscess formation was not observed in the ED99Δ*spsL*Δ*spsD*-
175 infected mice, which instead revealed cellulitis characterised by poorly delineated, regionally
176 extensive areas of suppurative inflammation accompanied by abundant necrotic debris, particularly
177 in the deeper cutaneous layers (Fig. 3C). The inflammatory infiltrate extended laterally between
178 tissue planes. Both distinct pathology types, abscessation and cellulitis, contained neutrophils as the
179 predominant inflammatory cell (Fig. 3C). No differences in spleen length or infection severity
180 between infection groups was recorded with wide within-group variation observed (Fig. S3A and
181 B). The categorisation of cellulitis correlated with larger histopathological lesions in

ED99Δ*spsL*Δ*spsD*-infected mice in comparison to wildtype-infected mice at both 2 ($p \leq 0.05$) and 3 dpi ($p \leq 0.0001$) (Fig. 3D). Categorising the histopathological changes into abscessation or cellulitis confirmed decreased abscess formation in ED99Δ*spsL*Δ*spsD*-infected mice ($p \leq 0.005$) (Fig. 3E). These data suggest that formation of a focal abscess after cutaneous inoculation in mice is dependent on expression of one or more CWA proteins.

SpsL is Required for the Development of Skin Abscesses in a Murine Infection Model. In order to investigate the relative role of SpsD and SpsL, single gene deletion mutants, ED99Δ*spsD* and ED99Δ*spsL*, were employed. Ten female BALB/c mice were inoculated with either wildtype, ED99Δ*spsD*, ED99Δ*spsL*, or ED99Δ*spsL*Δ*spsD* strains of *S. pseudintermedius* as described above, monitored, and euthanized at 1, 2, and 3 dpi. Measurement of body weight and cutaneous lesion length demonstrated that ED99Δ*spsD*-infected mice displayed characteristics more similar to the wildtype-infected mice, while both the ED99Δ*spsL*- and ED99Δ*spsL*Δ*spsD*-infected mice displayed decreased body weight (Fig. 4A), and increased lesion length ($p \leq 0.001$) (Fig 4B) in comparison to wildtype-infected mice. Although upon histopathological examination no differences in histopathology lesion length were identified (Fig. 4C), clear differences were observed in the type of histopathology present between experimental groups (Fig 4D). The wildtype- and ED99Δ*spsD*-infected mice were more likely to develop abscesses, and the ED99Δ*spsL*- and ED99Δ*spsL*Δ*spsD*-infected mice were more likely to develop cellulitis ($p \leq 0.01$) (Fig. 4D).

To confirm the role of SpsL in abscess formation and fulfil Molecular Koch's postulates (19), the *spsL* gene was re-introduced to the ED99Δ*spsL* strain by allele replacement as described in the Materials and Methods. The ED99Δ*spsL* Repaired (Rep) strain demonstrated restored SpsL surface expression and bacterial adherence to canine fibrinogen allowing analysis in the murine model alongside the wildtype and ED99Δ*spsL* strain using the same experimental setup as above (Fig. S4). Gross examination identified no differences in the body weight of mice from all experimental groups (Fig. 5A). However, there were raised, soft cutaneous lesions with a reddened

margin present at the inoculation site of the ED99Δ*spsL* Rep-infected mice similar to the wildtype-infected mice with the ED99Δ*spsL*-infected mice demonstrating flattened, cutaneous lesions that were significantly longer at 1 ($p \leq 0.05$) and 2 dpi ($p \leq 0.001$) (Fig. 5B). Histopathological examination confirmed that ED99Δ*spsL* Rep-infected mice were more likely to develop abscesses than ED99Δ*spsL*-infected mice ($p \leq 0.001$) (Fig. 5C). These data indicate that SpsL is the first *S. pseudintermedius* virulence factor to be described and that SpsL plays a key role in determining the pathology of *S. pseudintermedius* infection in this murine cutaneous model.

Cellulitis is Linked with Increased Bacterial Load. In order to quantify the number of viable bacteria associated with the two observed pathology types, the above experiment involving 4 experimental groups, was repeated. At 1, 2, and 3 dpi the mice were euthanised, the cutaneous lesion on the dorsal midline excised, homogenised, and cultured to determine the number of live bacteria present in the tissue (total CFU/lesion). The same gross observations were identified relating to larger lesions in ED99Δ*spsL*- and ED99Δ*spsL*Δ*spsD*-infected mice in comparison to wildtype- and ED99Δ*spsD*-infected mice (data not shown). In addition, increased bacterial load was identified in ED99Δ*spsL*- and ED99Δ*spsL*Δ*spsD*-infected mice in comparison to wildtype- and ED99Δ*spsD*-infected mice at 2 and 3 dpi ($p \leq 0.001$) (Fig. 6). Importantly, mice infected with a strain with a restored *spsL* gene, ED99Δ*spsL* Rep, had less bacteria present in the cutaneous lesion in comparison to ED99Δ*spsL*-infected mice at 1 ($p \leq 0.05$), 2 ($p \leq 0.001$), and 3 dpi ($p \leq 0.01$) and with similar numbers to wildtype-infected mice (Fig. 5D). These data reveal an association between pathology and bacterial burden that is dependent on SpsL.

Discussion

The global dissemination of multidrug resistant MRSP strains is making it increasingly difficult to treat canine pyoderma. There are also increasing reports of human-related infections caused by *S. pseudintermedius* and colonisation of veterinary staff (20-22). Similarly to dogs, skin and soft tissue infections, including abscess formation, are the most common form of disease caused by *S. pseudintermedius* in humans (20, 22). However, some more invasive infections have also been reported including bloodstream-infection and cellulitis (20, 23). If much-needed novel therapeutics are to be developed to combat MRSP then a greater understanding of the critical host-pathogen interactions leading to the development of canine pyoderma and human skin and soft tissue infections is required. Here we have established the first murine model of *S. pseudintermedius* skin infection. Subcutaneous injection of *S. pseudintermedius* ED99 led to the development of focal skin abscesses (Fig. 2B) similar to those observed after subcutaneous injection of *S. aureus* (24). We identified that while SpsD is dispensable, SpsL is required for the development of classic *S. pseudintermedius* skin abscesses in the murine model.

A common feature of *S. aureus* cutaneous infection models is the development of dermonecrosis, depending on the inoculum dose and bacterial strain used (16, 25). *S. aureus* dermonecrosis is dependent on toxins such as the α-toxin and the α-type phenol-soluble modulins, with mice infected with strains deficient in *hla* or *psmα* genes unable to develop dermonecrosis (26-28). No dermonecrosis was evident in this study but necrosis was identified that typically involved the epidermis but was also variably associated with underlying cutaneous layers. This necrosis of the epidermis was present in all experimental groups and was not associated with the development of a particular type of pathology. This demonstrates that the development of cellulitis is not linked with changes in the level of epidermal necrosis and that the dermonecrosis discussed in the *S. aureus* literature is not akin to the cellulitis phenotype described here.

Clinically, abscess formation and cellulitis are distinct phenotypes that can present simultaneously and can be both acute and chronic (24). Abscesses encase the bacteria in a confined location while cellulitis is more likely to affect a larger area of the skin with diffuse infiltrations of

256 neutrophils (29). The development of cellulitis in dogs is rare but cases of *S. pseudintermedius*-
257 mediated cellulitis have been reported with lymphatic damage linked to bacteraemia and toxic
258 shock or necrotising fasciitis (30-32). There is little understanding as to how either an abscess or
259 cellulitis pathology develops but it has been thought that the host immune response has a pivotal
260 role in driving the development of each pathology (29). The work presented here suggests that
261 bacterial surface proteins can determine the pathological outcome of infection.

262 For *S. aureus*-mediated skin abscesses or micro-abscesses, formed after bloodstream
263 infection, a number of bacterial proteins have been implicated in the development of abscesses (33).
264 The secreted coagulase and von Willebrand-binding protein (vWbp) are required for cutaneous
265 abscess formation in both mice and rabbits (34, 35). In addition, a sortase mutant lacking expression
266 of CWA proteins, as well as strains with deletions of particular genes, such as *clfA*, have been
267 employed to demonstrate the role of CWA proteins in the development of skin abscesses (16).
268 However, in contrast to what we observe with SpsL in the current study, loss of expression does not
269 lead to the development of a cellulitis pathology. These data suggest that SpsL exhibits a function
270 not previously observed among other staphylococcal surface proteins.

271 The most abundant extracellular matrix protein in healthy skin is collagen. However, when
272 skin is damaged, such as during subcutaneous inoculation, the initiation of the coagulation cascade
273 leads to platelet activation resulting in high levels of fibrinogen and fibronectin at the inoculation
274 site (36, 37). We postulate that SpsL promotes abscess formation through the development of a
275 fibrinogen- or fibronectin-shield on the bacterial surface that could initiate bacterial aggregation.
276 The importance of bacterial aggregation for the initial stages of skin abscess development has
277 already been reported for *S. aureus* with bacterial aggregates linked to increased bacterial load and
278 bacterial dissemination (38). In *S. aureus*, this aggregation is coagulase-dependent with a lack of
279 aggregation leading to decreased bacterial burden (38). In contrast, SpsL-dependent abscess
280 formation results in a decreased bacterial burden at 2 and 3 dpi in comparison to the alternative
281 cellulitis pathology (Fig. 6). The widespread conservation of the *spsL* gene in *S. pseudintermedius*

strains from across the world suggests that *S. pseudintermedius* could favour the development of subcutaneous abscesses rather than cellulitis (7, 13, 39, 40). Experiments performed over a longer period of time could identify if *S. pseudintermedius* were able to persist and avoid clearance in the SpsL-dependent abscesses in comparison to the cellulitis pathology. Additionally, bacterial aggregation could be beneficial to *S. pseudintermedius* in other types of infection and particularly in the initial stages of biofilm formation, which may promote colonisation and persistence on indwelling devices or atopic skin (41, 42).

Ideally, the role of SpsL in abscess formation and the mechanism involved could be further examined using a canine infection model. A canine superficial pyoderma model has been developed allowing the application of bacteria onto artificially created skin abrasions (43). This model produces classical clinical signs of pyoderma including the development of pustules and dermatitis that was self-limiting (43). It would be interesting to investigate the role of both SpsD and SpsL in this model as their role in cell invasion *in vivo* could also be established.

In conclusion, by developing the first *S. pseudintermedius* murine model, we have been able to examine the role of the 2 CWA proteins of *S. pseudintermedius*, SpsD and SpsL, in the development of cutaneous infections. We have identified that SpsL promotes the development of abscesses and this is the first description of a bacterial CWA protein influencing the type of cutaneous pathology developed during experimental infection. As so little is known about the immune mechanisms responsible for the development of either an abscess or cellulitis pathology, the model developed here could be useful for future investigations into the molecular basis of these clinical manifestations. More work into the *in vivo* function of virulence factors of *S. pseudintermedius* is needed if we aim to develop novel therapeutics to combat the increasingly multi-drug resistant clinical strains of *S. pseudintermedius*.

Materials and Methods

Ethics Statement. All murine experiments were carried out under the authority of a UK Home Office Project License (PPL 70/08663) within the terms and conditions of the strict regulations of the UK Home Office Animals (Scientific Procedures) Act 1986 and the code of practice for the housing and care of animals supplied for scientific purposes. In all experiments female BALB/cANCrl (Charles River, hereafter abbreviated as BALB/c) mice aged between 10-12 weeks were used. All mice were housed under specific pathogen-free (SPF) conditions at the Biological Research Facility (BRF) for rodents at the Roslin Institute according to hygiene recommendations of Federation of European Laboratory Animal Science Associations (FELASA) guidelines (44, 45). Mice were randomly assigned to individually ventilated home cages after arrival and acclimatised for 1 to 2 weeks in the facility before being used in infection challenge studies. Animals had, throughout maintenance and infection challenge, *ad libitum* access to food and water. Mice were maintained on a standard diet (Teklad Global 18% Protein Rodent Diet), at an average room temperature of 21°C and a 12:12 h light/dark cycle. All study protocols were reviewed by the Roslin Institute (University of Edinburgh) animal services, consisting of the named veterinary surgeon (NVS), the rodent facility director, and a senior research statistician, prior to each experiment. Animals were monitored twice daily to ensure that no animal exceeded agreed euthanasia criteria including a 20% loss of body weight or moderate signs of general illness. Only mild symptoms of generalised illness were noted with slight decreases in weight, some discharge from the eyes, and starring of the fur. No animal required premature euthanasia with all animals humanely euthanized at the end of experimentation by schedule 1 asphyxiation using carbon dioxide (VetTech Solutions). Euthanized animals were then subjected to cervical dislocation to ensure euthanasia.

Solid Phase Adherence Assays. Solid phase adherence assays were performed as described previously (13). Briefly, murine fibrinogen (Abcam), murine fibronectin (Abcam), or recombinant murine cytokeratin-10 C-terminus (294-570) (purified as described previously (46)) were coated overnight at 4°C in PBS on 96-well MaxiSorp® plates (Nunc). Wells were blocked with 100 µl 8%

(w/v) non-fat dried milk (Fluka Analytical) for 2 h at 37°C. *Lactococcus lactis* strains, characterised previously (13), were cultured overnight in M17 broth (Oxoid), washed in PBS and diluted to an OD_{600} of 1.0 in PBS. *S. pseudintermedius* strains, characterised previously (15), were cultured in Brain Heart Infusion broth (Oxoid) until an OD_{600} of 0.6, washed in PBS and diluted to an OD_{600} of 1.0 in PBS. Bacteria were applied to the wells in triplicate and incubated for 2 h at 30°C for *L. lactis*, or 2 h at 37°C for *S. pseudintermedius*. Bound bacteria were fixed with 100 µl 25% (v/v) formaldehyde (Sigma-Aldrich) for 30 min and then stained with 50 µl 0.5% (w/v) crystal violet (Sigma-Aldrich) for 3 min. Before analysis, 5% (v/v) acetic acid (BDH Lab Supplies) was applied and the plate read using a Synergy™ HT plate reader (BioTek) at a wavelength of 590 nm.

Murine Skin Infection Model. The bacterial inoculum was produced by culturing *S. pseudintermedius* strains to an OD_{600} of 0.6 in Brain Heart Infusion broth (Oxoid). 10 ml of culture was washed and then diluted in PBS to the relevant OD_{600} to provide 10^7 colony forming units (CFU) per 100 µl. The size of the inoculum used for infection challenge was confirmed by CFU plating for each experiment.

The dorsal midline of isoflurane anaesthetised BALB/c mice were shaved using electric clippers 24 h pre-inoculum. Bacteria were injected into the subcutaneous tissue of the dorsal midline just caudal to the intrascapular region of the BALB/c mouse in 100 µl volume using a 26-gauge needle and a 5 mm needle guard to ensure standard injection depths. Mice were caged with 6 or less mice per cage with at least 6 mice per experimental group. All animals were monitored for weight, length of observed lesion along the longest axis using callipers, noting the presence or absence of a lump, as well as identifying any clinical signs of illness. Measuring the longest axis of the lesion was deemed the most appropriate measure as the lesions developed were highly irregular in shape meaning that measurement of lesion width was very subjective. Mice were humanely euthanized at 1, 2, 3, or 4 days post-infection (dpi). Spleens and skin lesions were immediately excised and immersed in 10% formal buffered saline (Fisher Scientific) for histopathological analysis. All experiments were repeated at least twice giving the same results.

Skin lesions were trimmed and histopathology slides produced by the Pathology Department of the Royal Dick School of Veterinary Studies, University of Edinburgh using routine methods. Histology slides were stained with hematoxylin and eosin (H&E) giving nuclei a blue staining and proteinaceous material a pink staining. Histopathology slides were analysed blind for lesion length along the longest axis using a magnifying glass and callipers, as well as disease severity and categorised depending on the type of pathology present (abscess/cellulitis). This analysis was independently performed by two persons before unblinding. All histopathology slides included for analysis contained the following 5 layers of skin: epidermis, dermis, panniculus, panniculus carnosus muscle, and adventitia. Histopathology slides were removed from the analysis if only superficial layers of the skin were present on the slide.

For colony forming units (CFU) determination, after excision of the skin lesion, the area was sliced into equal sections using a scalpel. These skin sections (containing the whole of the skin lesion) were suspended in 1 ml PBS in Lysing Matrix D tubes containing 1.4 mm ceramic spheres (MP Bio). After calculating the weight of the skin lesion, homogenisation of the skin samples were performed by pulsing the samples at 4.0 m/sec twice for 20 s per pulse with a minute break between pulses. Triplicate serial dilutions were produced per homogenate and plated for CFU enumeration.

Histopathology Severity Scoring. The overall severity of pathology present on the histopathology slide was scored using the following system: grade 0, minimal pathological changes; grade 1, mild inflammatory changes with a mild increase in the number of neutrophils and lymphocytes present in the panniculus and deeper connective tissue layers; grade 2, moderate pathology with formation of either a focal, well-defined abscess in the skin accompanied by inflammation in surrounding tissues or a laterally-oriented cellulitis with a poorly defined accumulation of neutrophils and cell debris extending between the tissue planes; grade 3, marked pathology displaying more extensive pathology with the abscess or cellulitis effacing a larger area of the section and overlying epidermal ulceration often noted; and grade 4, severe pathology with

large abscess or cellulitis formation, epidermal ulceration, and disruption of normal tissue architecture.

Generation of ED99Δ*spsL* Repaired Strain. Sequence ligase independent cloning was used to clone the full length *spsL* gene, along with 500 bp flanking regions, into the temperature-sensitive allele replacement vector pIMAY as previously described (47, 48). A synonymous mutation was introduced into the N-terminal region of the *spsL* gene to allow identification in comparison to the wildtype (primer sequences are given in Table S1). The pIMAY plasmid containing the mutated *spsL* gene was electro-transformed into the *S. pseudintermedius* ED99Δ*spsL* background at 28°C with selection on 10 µg/ml chloramphenicol. Growth at 37°C selected for plasmid integration before plasmid excision at 28°C. The anti-sense *secY* mechanism was found to be non-functional in *S. pseudintermedius* as previously described (15). The generation of the ED99Δ*spsL* Rep strain was confirmed by PCR and Sanger sequencing as well as Western blot analysis. CWA protein profiles of strains cultured to an OD_{600} of 0.6 in Brain Heart Infusion broth, produced as described previously (15), were probed with 1 µg/ml anti-SpsL N2N3 IgY and 0.5 µg/ml F(ab')2 rabbit anti-chicken HRP-conjugated IgG (Bethyl Laboratories).

Statistical Analysis. Prism 6 (GraphPad) was employed to present data with statistical analysis performed using Minitab 16. The data of each experiment and each time point was analysed separately with data between time points not pooled except to analyse the pathology type data. The Anderson-darling test was used to assess data normality and equal variance. Data transformation was performed if required and analysed using either a 2-sample unpaired t-test or one-way ANOVA analysis with multiple comparisons performed when appropriate. If the data could not be successfully transformed, nonparametric analysis was performed including Kruskal Wallis or Mann-Whitney U test analysis. For analysis of severity grading, ordinal logistic regression was performed with pathology type data being analysed in pairs using Fisher's exact

analysis. For data displaying statistical significance: * represents $p \leq 0.05$, ** represents $p \leq 0.01$, and *** represents $p \leq 0.001$.

Acknowledgements

The authors would like to thank the following members of staff in the Roslin BRF for excellent animal care that was instrumental for this work: Fraser Laing, Darren Smith, Elizabeth Blackford, Christine Marshall, and Dave Davies. We thank Dr. Jane Gebbie and Dr. Amanda Novak for veterinary advice on infection studies and Dr. Helen Brown for advice and help with statistical analysis. We are grateful for funding from Zoetis Animal Health and the Biotechnology and Biological Sciences Research Council (BBSRC). The work was partly supported by the BBSRC Institute Strategic Program Funding (BBS/E/D/20231761, BBS/E/D/20231762, and BBS/E/D/20002173) provided to J. R. F., and A. L. The protein studied is subject of a patent (US9879054B2).

Author contributions for this study were as follows. Experiments were conceived by: A.L., J.R.F., A.C.R., and performed and analysed by: A.C.R., M.O., S.W.T., M.I.G., P.M.B. The manuscript was written by A.C.R., P.M.B., A.L., J.R.F, and reviewed by all authors.

References

1. **Bannoehr J, Guardabassi L.** 2012. *Staphylococcus pseudintermedius* in the dog: taxonomy, diagnostics, ecology, epidemiology and pathogenicity. Veterinary Dermatology **23:**119-124.
2. **Hillier A, Griffin CE.** 2001. The ACVD task force on canine atopic dermatitis (I): incidence and prevalence. Veterinary Immunology and Immunopathology **81:**147-151.
3. **Hillier A, Lloyd DH, Weese JS, Blondeau JM, Boothe D, Breitschwerdt E, Guardabassi L, Papich MG, Rankin S, Turnidge JD, Sykes JE.** 2014. Guidelines for the diagnosis and antimicrobial therapy of canine superficial bacterial folliculitis. Veterinary Dermatology **25:**163-175.
4. **Horvath C, Neuber A.** 2007. Management of canine pyoderma. Companion Animal **12:**55-64.

5. **Ruscher C, Lübke-Becker A, Semmler T, Wleklinski C-G, Paasch A, Šoba A, Stamm I, Kopp P, Wieler LH, Walther B.** 2010. Widespread rapid emergence of a distinct methicillin- and multidrug-resistant *Staphylococcus pseudintermedius* (MRSP) genetic lineage in Europe. Veterinary Microbiology **144:**340-346.
6. **Moodley A, Damborg P, Nielsen SS.** 2014. Antimicrobial resistance in methicillin susceptible and methicillin resistant *Staphylococcus pseudintermedius* of canine origin: Literature review from 1980 to 2013. Veterinary Microbiology **171:**337-341.
7. **McCarthy AJ, Harrison EM, Stanczak-Mrozek K, Leggett B, Waller A, Holmes MA, Lloyd DH, Lindsay JA, Loeffler A.** 2015. Genomic insights into the rapid emergence and evolution of MDR in *Staphylococcus pseudintermedius*. The Journal of Antimicrobial Chemotherapy **70:**997-1007.
8. **Hensel N, Zabel S, Hensel P.** 2016. Prior antibacterial drug exposure in dogs with meticillin-resistant *Staphylococcus pseudintermedius* (MRSP) pyoderma. Veterinary Dermatology **27:**72-e20.
9. **Futagawa-Saito K, Makino S, Sunaga F, Kato Y, Sakurai-Komada N, Ba-Thein W, Fukuyasu T.** 2009. Identification of first exfoliative toxin in *Staphylococcus pseudintermedius*. FEMS Microbiology Letters **301:**176-180.
10. **Iyori K, Futagawa-Saito K, Hisatsune J, Yamamoto M, Sekiguchi M, Ide K, Son W-G, Olivry T, Sugai M, Fukuyasu T, Iwasaki T, Nishifuji K.** 2011. *Staphylococcus pseudintermedius* exfoliative toxin EXI selectively digests canine desmoglein 1 and causes subcorneal clefts in canine epidermis. Veterinary Dermatology **22:**319-326.
11. **Iyori K, Hisatsune J, Kawakami T, Shibata S, Murayama N, Ide K, Nagata M, Fukata T, Iwasaki T, Oshima K, Hattori M, Sugai M, Nishifuji K.** 2010. Identification of a novel *Staphylococcus pseudintermedius* exfoliative toxin gene and its prevalence in isolates from canines with pyoderma and healthy dogs. FEMS Microbiology Letters **312:**169-175.
12. **Simou C.** 2005. Adherence of *Staphylococcus intermedius* to corneocytes of healthy and atopic dogs: effect of pyoderma, pruritus score, treatment and gender. Veterinary Dermatology **16:**352-361.
13. **Bannoehr J, Ben Zakour NL, Reglinski M, Inglis NF, Prabhakaran S, Fossum E, Smith DG, Wilson GJ, Cartwright RA, Haas J, Hook M, van den Broek AH, Thoday KL, Fitzgerald JR.** 2011. Genomic and surface proteomic analysis of the canine pathogen *Staphylococcus pseudintermedius* reveals proteins that mediate adherence to the extracellular matrix. Infection and Immunity **79:**3074-3086.
14. **Pietrocola G, Geoghegan JA, Rindi S, Di Poto A, Missineo A, Consalvi V, Foster TJ, Speziale P.** 2013. Molecular Characterization of the Multiple Interactions of SpsD, a Surface Protein from *Staphylococcus pseudintermedius*, with Host Extracellular Matrix Proteins. PLoS ONE **8:**e66901.
15. **Pietrocola G, Gianotti V, Richards A, Nobile G, Geoghegan JA, Rindi S, Monk IR, Bordt AS, Foster TJ, Fitzgerald JR, Speziale P.** 2015. Fibronectin binding proteins SpsD and SpsL both support invasion of canine epithelial cells by *Staphylococcus pseudintermedius*. Infection and Immunity **83:**4093-4102.
16. **Kwiecinski J, Jin T, Josefsson E.** 2014. Surface proteins of *Staphylococcus aureus* play an important role in experimental skin infection. APMIS **122:**1240-1250.
17. **Liu Q, Du X, Hong X, Li T, Zheng B, He L, Wang Y, Otto M, Li M.** 2015. Targeting Surface Protein SasX by Active and Passive Vaccination To Reduce *Staphylococcus aureus* Colonization and Infection. Infection and Immunity **83:**2168-2174.
18. **Patel AH, Nowlan P, Weavers ED, Foster T.** 1987. Virulence of protein A-deficient and alpha-toxin-deficient mutants of *Staphylococcus aureus* isolated by allele replacement. Infection and Immunity **55:**3103-3110.
19. **Falkow S.** 1988. Molecular Koch's Postulates Applied to Microbial Pathogenicity. Review of Infectious Diseases **10:**274-276.
20. **Somayaji R, Priyantha MAR, Rubin JE, Church D.** 2016. Human infections due to *Staphylococcus pseudintermedius*, an emerging zoonosis of canine origin: report of 24 cases. Diagnostic Microbiology and Infectious Disease **85:**471-476.
21. **Feßler AT, Schuenemann R, Kadlec K, Hensel V, Brombach J, Murugaiyan J, Oechtering G, Burgener IA, Schwarz S.** 2018. Methicillin-resistant *Staphylococcus aureus* (MRSA) and methicillin-

resistant *Staphylococcus pseudintermedius* (MRSP) among employees and in the environment of a small animal hospital. Veterinary Microbiology **221:**153-158.

22. **Lee J, Murray A, Bendall R, Gaze W, Zhang L, Vos M.** 2015. Improved Detection of *Staphylococcus intermedius* Group in a Routine Diagnostic Laboratory. Journal of Clinical Microbiology **53:**961-963.
23. **Carmen L, Antonio R, Isabel F, Vanesa P-L, Myriam Z, Laura R-R, José RM, Carmen T.** 2017. *Staphylococcus pseudintermedius* Human Infection Cases in Spain: Dog-to-Human Transmission. Vector-Borne and Zoonotic Diseases **17:**268-270.
24. **Kobayashi SD, Malachowa N, DeLeo FR.** 2015. Pathogenesis of *Staphylococcus aureus* Abscesses. The American Journal of Pathology **185:**1518-1527.
25. **Bunce C, Wheeler L, Reed G, Musser J, Barg N.** 1992. Murine model of cutaneous infection with gram-positive cocci. Infection and Immunity **60:**2636-2640.
26. **Kennedy AD, Wardenburg JB, Gardner DJ, Long D, Whitney AR, Braughton KR, Schneewind O, DeLeo FR.** 2010. Targeting of Alpha-Hemolysin by Active or Passive Immunization Decreases Severity of USA300 Skin Infection in a Mouse Model. Journal of Infectious Diseases **202:**1050-1058.
27. **Kobayashi SD, Malachowa N, Whitney AR, Braughton KR, Gardner DJ, Long D, Wardenburg JB, Schneewind O, Otto M, DeLeo FR.** 2011. Comparative Analysis of USA300 Virulence Determinants in a Rabbit Model of Skin and Soft Tissue Infection. Journal of Infectious Diseases **204:**937-941.
28. **Wang R, Braughton KR, Kretschmer D, Bach T-HL, Queck SY, Li M, Kennedy AD, Dorward DW, Klebanoff SJ, Peschel A, DeLeo FR, Otto M.** 2007. Identification of novel cytolytic peptides as key virulence determinants for community-associated MRSA. Nature Medicine **13:**1510-1514.
29. **Bailey E, Kroshinsky D.** 2011. Cellulitis: diagnosis and management. Dermatologic Therapy **24:**229-239.
30. **Girard C, Higgins R.** 1999. *Staphylococcus intermedius* cellulitis and toxic shock in a dog. The Canadian Veterinary Journal **40:**501-502.
31. **Weese JS, Poma R, James F, Buenviaje G, Foster R, Slavic D.** 2009. *Staphylococcus pseudintermedius* necrotizing fasciitis in a dog. The Canadian Veterinary Journal **50:**655-656.
32. **Mayer MN, Rubin JE.** 2012. Necrotizing fasciitis caused by methicillin-resistant *Staphylococcus pseudintermedius* at a previously irradiated site in a dog. The Canadian Veterinary Journal **53:**1207-1210.
33. **Cheng AG, DeDent AC, Schneewind O, Missiakas D.** 2011. A play in four acts: *Staphylococcus aureus* abscess formation. Trends in Microbiology **19:**225-232.
34. **Vanassche T, Verhaegen J, Peetermans WE, Van Ryn J, Cheng A, Schneewind O, Hoylaerts MF, Verhamme P.** 2011. Inhibition of staphylothrombin by dabigatran reduces *Staphylococcus aureus* virulence. Journal of Thrombosis and Haemostasis **9:**2436-2446.
35. **Malachowa N, Kobayashi SD, Porter AR, Braughton KR, Scott DP, Gardner DJ, Missiakas DM, Schneewind O, DeLeo FR.** 2016. Contribution of *Staphylococcus aureus* Coagulases and Clumping Factor A to Abscess Formation in a Rabbit Model of Skin and Soft Tissue Infection. PLOS ONE **11:**e0158293.
36. **Chester D, Brown AC.** 2017. The role of biophysical properties of provisional matrix proteins in wound repair. Matrix Biology **60-61:**124-140.
37. **Rousselle P, Montmasson M, Garnier C.** 2018. Extracellular matrix contribution to skin wound re-epithelialization. Matrix Biology
38. **Loof TG, Goldmann O, Naudin C, Mörgelin M, Neumann Y, Pils MC, Foster SJ, Medina E, Herwald H.** 2015. *Staphylococcus aureus*-induced clotting of plasma is an immune evasion mechanism for persistence within the fibrin network. Microbiology **161:**621-627.
39. **Maali Y, Martins-Simões P, Valour F, Bouvard D, Rasigade J-P, Bes M, Haenni M, Ferry T, Laurent F, Trouillet-Assant S.** 2016. Pathophysiological Mechanisms of *Staphylococcus* Non-*aureus* Bone and Joint Infection: Interspecies Homogeneity and Specific Behavior of *S. pseudintermedius*. Frontiers in Microbiology **7**.
40. **Phumthanakorn N, Chanchaithong P, Prapasarakul N.** 2017. Development of a set of multiplex PCRs for detection of genes encoding cell wall-associated proteins in *Staphylococcus*

pseudintermedius isolates from dogs, humans and the environment. Journal of Microbiological Methods **142:**90-95.

41. **Vanassche T, Peetermans M, Van Aelst LNL, Peetermans WE, Verhaegen J, Missiakas DM, Schneewind O, Hoylaerts MF, Verhamme P.** 2013. The role of staphylothrombin-mediated fibrin deposition in catheter-related *Staphylococcus aureus* infections. Journal of Infectious Diseases **208:**92-100.
42. **Gonzalez T, Biagini Myers JM, Herr AB, Khurana Hershey GK.** 2017. Staphylococcal Biofilms in Atopic Dermatitis. Current Allergy and Asthma Reports **17:**81.
43. **Bäumer W, Bizikova P, Jacob M, Linder KE.** 2017. Establishing a canine superficial pyoderma model. Journal of Applied Microbiology **122:**331-337.
44. **Guillen J.** 2012. FELASA Guidelines and Recommendations. Journal of the American Association for Laboratory Animal Science : JAALAS **51:**311-321.
45. **rodents Fwgorogfhmo, rabbits, Mähler M, Berard M, Feinstein R, Gallagher A, Illgen-Wilcke B, Pritchett-Corning K, Raspa M.** 2014. FELASA recommendations for the health monitoring of mouse, rat, hamster, guinea pig and rabbit colonies in breeding and experimental units. Laboratory Animals **48:**178-192.
46. **Walsh EJ, O'Brien LM, Liang X, Hook M, Foster TJ.** 2004. Clumping Factor B, a Fibrinogen-binding MSCRAMM (Microbial Surface Components Recognizing Adhesive Matrix Molecules) Adhesin of *Staphylococcus aureus*, Also Binds to the Tail Region of Type I Cytokeratin 10. Journal of Biological Chemistry **279:**50691-50699.
47. **Monk IR, Tree JJ, Howden BP, Stinear TP, Foster TJ.** 2015. Complete Bypass of Restriction Systems for Major *Staphylococcus aureus* Lineages. mBio **6:**e00308.
48. **Li MZ, Elledge SJ.** 2007. Harnessing homologous recombination in vitro to generate recombinant DNA via SLIC. Nat Meth **4:**251-256.

Figure Legends

FIG 1 SpsD and SpsL promote adherence to murine fibronectin, fibrinogen, and cytokeratin-10. Bacterial solid phase adherence assays of stationary phase (A) *L. lactis* expressing SpsD, and (B) *L. lactis* expressing SpsL to murine fibronectin, fibrinogen, and cytokeratin-10. Bacterial solid phase adherence assays of ED99 wildtype (WT) (closed circle), ED99Δ*spsD* (open square), ED99Δ*spsL* (closed triangle), and ED99Δ*spsL*Δ*spsD* (open triangle) to (C) murine fibronectin, (D) murine fibrinogen, and (E) murine cytokeratin-10 at early exponential growth phase (OD_{600} of 0.2). Each data point represents the mean value from three independent experiments; error bars represent SD.

FIG 2 *S. pseudintermedius* ED99-infected mice develop skin abscesses. Monitoring data is shown as (A) percentage change in body weight and (B) surface lesion length (mm) for ED99 wildtype (WT)-infected mice (black circle) and PBS-control mice (open triangle). Each data point represents

an individual mouse. Mean scores (horizontal bars) were analysed by two-sample unpaired t-test, *p≤0.05 and **p≤0.01. (C and D) Representative images of H&E-stained skin sections of a PBS-control mouse and a WT-infected mouse at 4 dpi. A hair follicle and all 5 layers of the skin are labelled in the PBS-control section. The WT section contains a large, well circumscribed abscess in the deeper layers of the skin. The abscess is composed of a necrotic centre surrounded by a concentric ring of neutrophils and cellular debris, and accompanied by suppurative dermatitis, panniculitis, myositis, and myofibre degeneration.

FIG 3 Infection with *S. pseudintermedius* ED99 deficient in SpsD and SpsL leads to the development of large surface lesions and cellulitis. Monitoring data is shown as (A) percentage change in body weight and (B) surface lesion length (mm) for WT- (black circle) and ED99Δ*spsL*Δ*spsD*-infected mice (open circle). Each data point represents an individual mouse and data are representative of a single replicate of experiments performed twice. Mean scores (horizontal bars) were analysed by two-sample unpaired t-test. (C) Representative images of H&E-stained skin sections of WT-infected or ED99Δ*spsL*Δ*spsD*–infected mice at 3 dpi. The WT-infected mice display a focal abscess. The ED99Δ*spsL*Δ*spsD*–infected mice display a horizontally oriented inflammation throughout the panniculus carnosus muscle layer akin to cellulitis. Magnification (by 100x) of the areas indicated by black rectangles demonstrate that regions of inflammation are composed predominantly of degenerate neutrophils admixed with cellular debris, in all experimental groups. (D) Histopathology lesion length (mm). (E) Number of mice demonstrating each pathology type. No abscesses were documented in the ED99Δ*spsL*Δ*spsD*–infected mice and the inflammation present is more longitudinally extended than in WT-infected mice. Fisher's exact analysis demonstrates differences in infection outcome between WT- and ED99Δ*spsL*Δ*spsD*-infected mice. Significant results are represented as * p≤0.05, **p≤0.01 and ***p≤0.001.

FIG 4 SpsL is required for *S. pseudintermedius* abscess formation. Monitoring data is shown as (A) percentage change in body weight and (B) surface lesion length (mm) for WT- (filled circle), ED99Δ*spsL*Δ*spsD*- (open circle), ED99Δ*spsD*- (filled square), or ED99Δ*spsL*-infected mice (open square). Each data point represents an individual mouse and data are representative of a single replicate of experiments performed twice. Mean scores (horizontal bars) were analysed by one-way ANOVA. (C) Histopathology lesion length (mm) was analysed by Kruskal-Wallis. (D) The number of mice demonstrating each pathology type. Fisher's exact analysis demonstrates differences in infection outcome between each experimental group compared to every other experimental group. Significant results are represented as * $p \leq 0.05$, ** $p \leq 0.01$ and *** $p \leq 0.001$.

FIG 5 Reintroduction of *spsL* to *S. pseudintermedius* restores the abscess phenotype. (A) Percentage change in body weight. Mean scores (horizontal bars) were analysed by one-way ANOVA. (B) Histopathology lesion length (mm). Mean scores were analysed by Kruskal-Wallis. (C) The number of mice demonstrating each pathology type. Fisher's exact analysis demonstrates differences in infection outcome between each experimental group compared to every other experimental group. (D) Log CFU/lesion. Mean values were analysed by one-way ANOVA with Tukey's multiple comparison analysis. Each data point represents an individual mouse with WT- (filled circle), ED99Δ*spsL*- (open square), or ED99Δ*spsL* Rep-infected mice (filled triangle). Significant results are represented as * $p \leq 0.05$, ** $p \leq 0.01$, and *** $p \leq 0.001$.

FIG 6 The cellulitis pathology induced by *S. pseudintermedius* deficient in SpsL is associated with increased bacterial numbers. The number of CFU were analysed after homogenisation of the excised and trimmed skin lesion. The logged CFU/lesion data is plotted with each data point representing an individual mouse for WT- (filled circle), ED99Δ*spsL*Δ*spsD*- (open circle),

ED99Δ*spsD*- (filled square), or ED99Δ*spsL*-infected mice (open square). Mean values (horizontal bar) were analysed by one-way ANOVA with Tukey's multiple comparison analysis, **p≤0.01, and ***p≤0.001. Mice infected with bacterial strains lacking the *spsL* gene have increased bacterial burdens at 2 and 3 dpi.

FIG 1

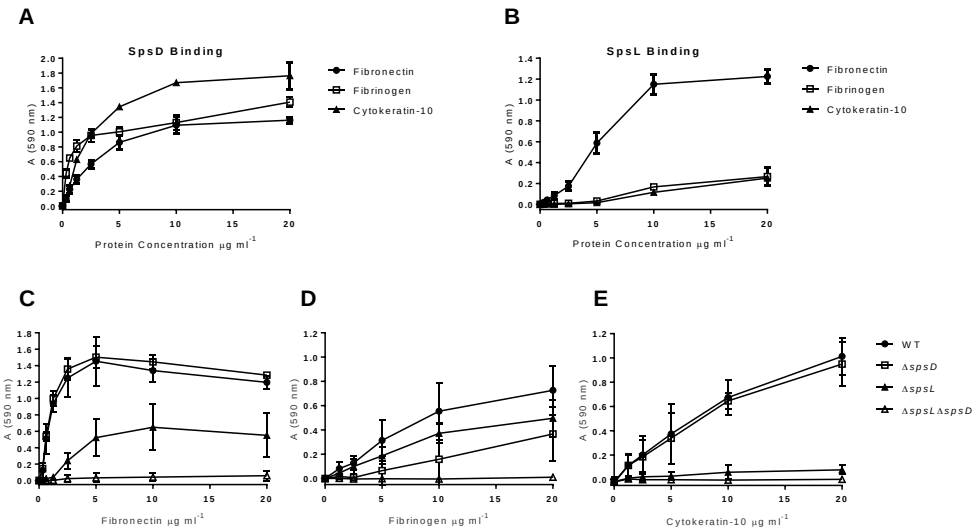

639

640

641

642

643

644

645

646

647

648 **FIG 2**

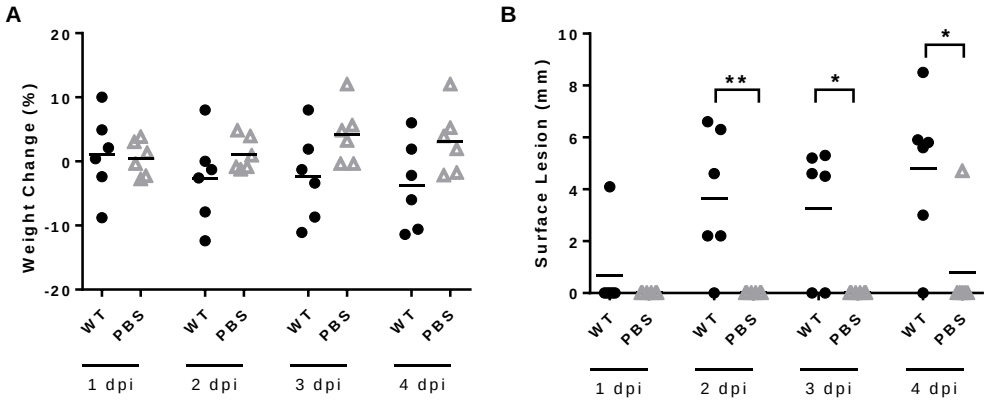

649

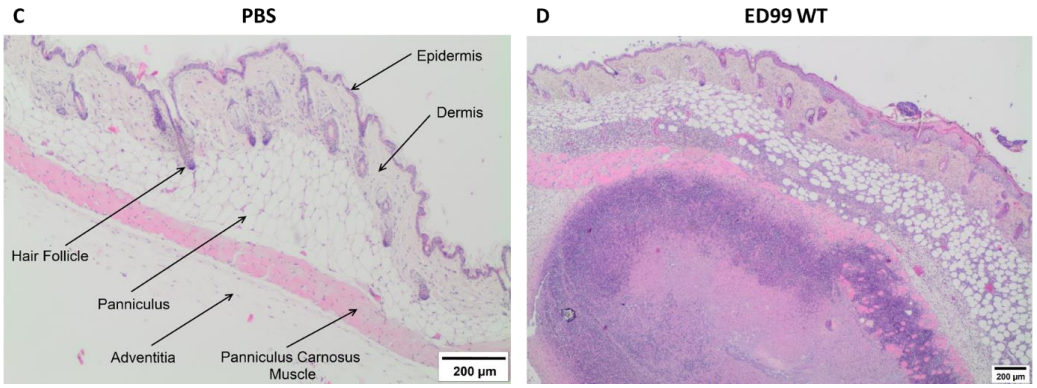

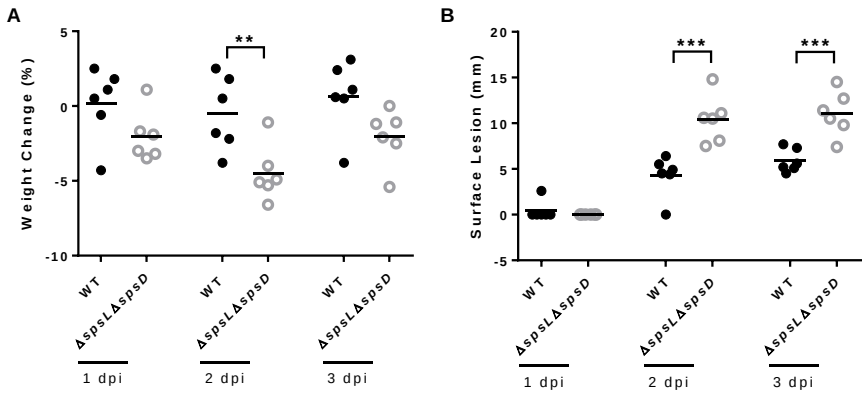

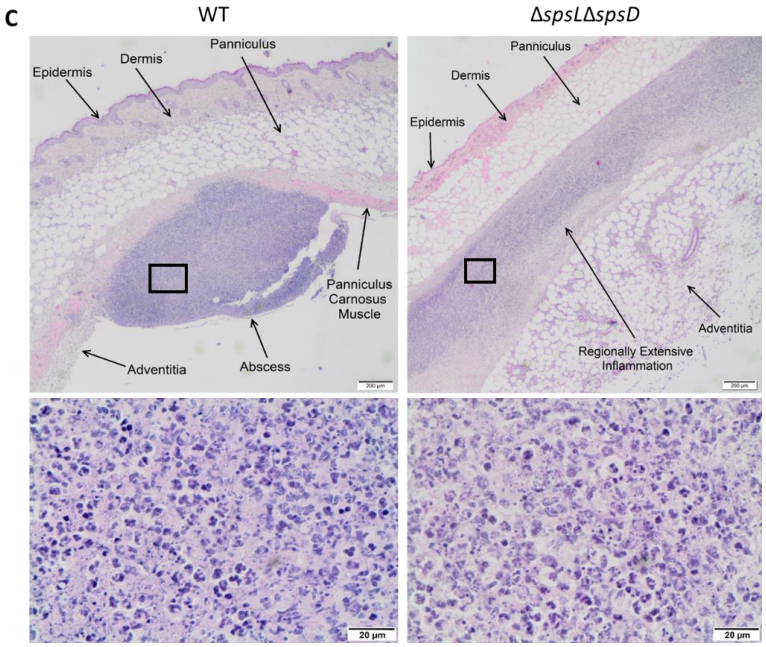

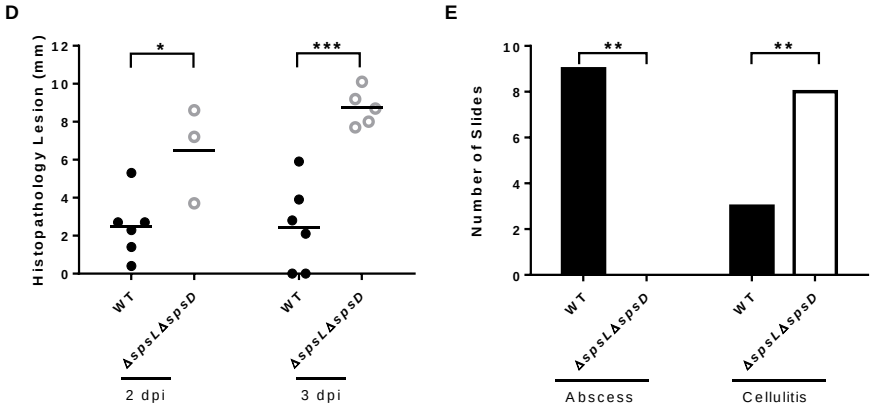

660

661 **FIG 4**

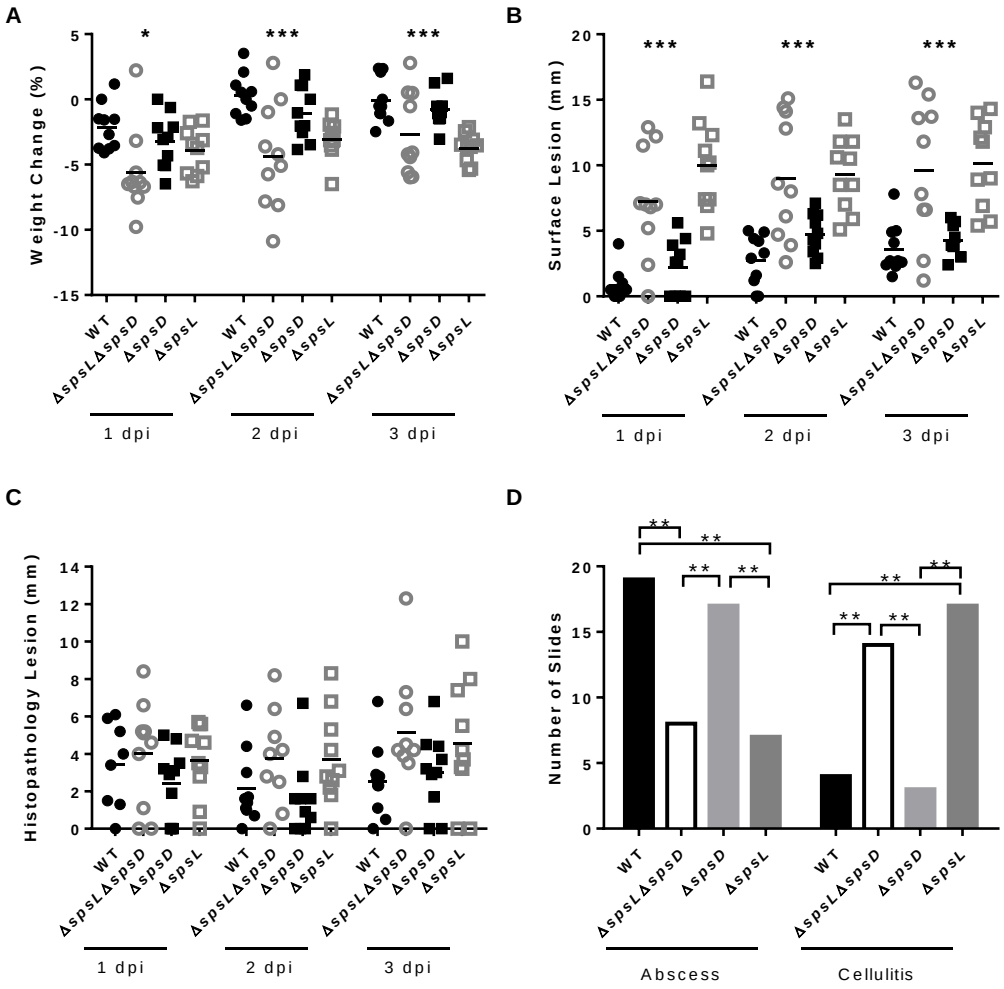

FIG 5

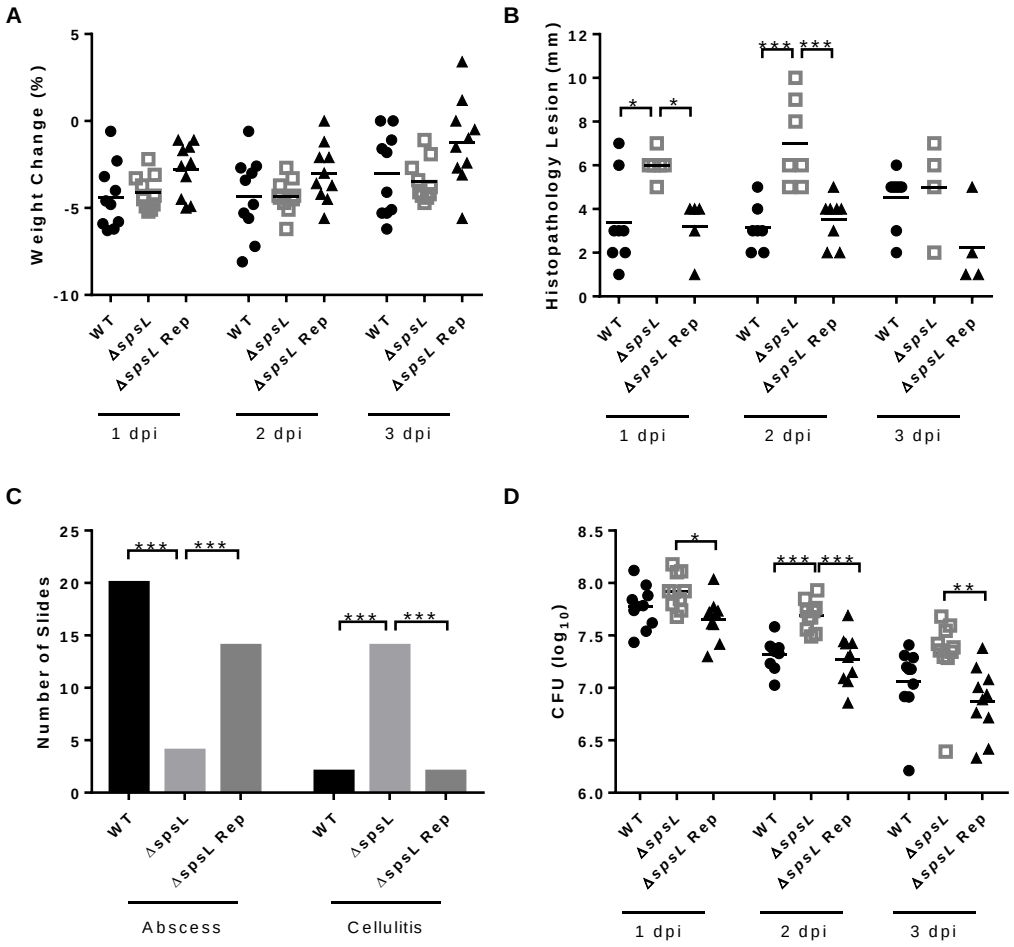

671

672

673

674

675

676

677

678

679 **FIG 6**

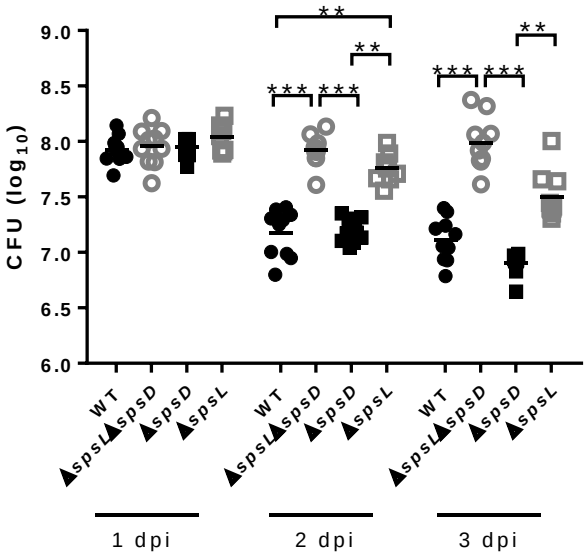

680

681

682